Microscopic mechanism of leakage currents in silica junctions

Xin Luo, Biao Wang' , and Yue Zheng

Citation: Journal of Applied Physics **106**, 073711 (2009); doi: 10.1063/1.3236640
View online: http://dx.doi.org/10.1063/1.3236640
View Table of Contents: http://aip.scitation.org/toc/jap/106/7
Published by the American Institute of Physics

Microscopic mechanism of leakage currents in silica junctions

Xin Luo,[1,2] Biao Wang,[1,a)] and Yue Zheng[1,2]
[1]*State and Key Laboratory of Optoelectronic Materials and Technologies, Institute of Optoelectronic and Functional Composite Materials and School of Physics and Engineering, Sun Yat-Sen University, Guangzhou 510275, China*
[2]*Department of Electronic and Information Engineering, The Hong Kong Polytechnic University, Hong Kong Special Administrative Region, China*

(Received 2 July 2009; accepted 25 August 2009; published online 9 October 2009)

Combining the nonequilibrium Green's functions with the density-functional theory, we investigated the structural and electronic properties of silica junctions sandwiched between Al electrodes. The results show that the oxygen vacancies and tensile strain field play an important role in the electron transport properties of these two-probe systems. Sizable changes in leakage current across the barrier are found for the oxygen deficient system. It is found that Si dangling bonds formed by the introduction of oxygen vacancies are the main building blocks of the conduction channel in silica thin film. The midband gap states generated by the Si dangling bonds contribute to the leakage current. Detail analysis shows that four conduction channels are generated in silica junction after the presence of oxygen vacancies, resulting in a large enhancement of the electron transmission coefficient at the Fermi level. This leakage current mechanism provides useful information in the microelectronic designs. © *2009 American Institute of Physics*. [doi:10.1063/1.3236640]

With the continual decrease in electronic device size, the thickness of dielectric oxide in a metal-insulator-metal capacitor is approaching a few nanometers.[1,2] One of the formidable challenges in drastic downscaling is the large leakage current tunneling through dielectric layers such as SiO_2, which resulted in disruptive components in the switchable circuit.[3] To reduce the leakage current, new materials such as high K material and metal gate are introduced in the microelectronic industry.[4,5] Since the high K gate oxide has a larger dielectric constant, replacing the SiO_2 gate oxide with high K material would allow the gate oxide to increase its capacitance without having to reduce its thickness. Under external field, both the traditional SiO_2 and new high K material will face the large leakage current problem when their thickness decreases to a few nanometers.[6] Thus it is an urgent and formidable task to understand the microscopic origin of the large leakage current and find the corresponding methods to tackle it.

Besides the high field intrinsic breakdown,[7] the SiO_2 will experience low field defect-related soft breakdown at low voltage bias, transiting from insulating to partially conductive.[8] It is believed that an electrical conductive path[9] will form and penetrate through the SiO_2 thin film when external electric field stresses beyond its dielectric strength, which is a sensitive property of SiO_2 insulator. Experimentally, many factors, such as the configuration of insulator, active interface defects, and the contacting electrodes, can influence the leakage current of the capacitor device.

Up to now, great efforts have been devoted to the evolution of dielectric leakage current,[5,10–12] and several dielectric breakdown models[13–18] have been put forward to explain the disruptive phenomenon observed in experiment. However, most of their studies are from the continual dielectric thermodynamics, which acts perfectly in the macroscopic and mesoscopic systems. While at nanometer scale, the quantum effects are dominant, and therefore quantum mechanical method should be used to elucidate the behaviors and properties of material in nanoelectronic devices. Many new physics appear in nanoscale capacitor due to the coupling effects of insulating barriers and the electrodes.[19,20] In order to understand the microscopic origin of the detrimental trapping defects, the large leakage current, and their influence on dielectric breakdown process, we combine nonequilibrium Green's function technique with density functional theory (DFT) to provide a physical analysis of the leakage current in the atomic scenario. The effects of interface structure, external stress, and defect trapping on electronic transport properties for the $Al-SiO_2-Al$ two-probe systems are reported in this study.

Figure 1 shows our model of $Al-SiO_2-Al$ system, which can be divided into left electrode, the scattering region, and the right electrode. The electronic and atomic structures of the electrodes are assumed to be the same as those of the bulk Al. On the other hand, the electronic states of the scattering region are calculated self-consistently. The scattering region consists of seven SiO_2 layers and four surface layers of the left and right electrodes. Oxygen vacancies (V_O) have been identified as an important factor in the formation of electron traps in many experimental researches.[21–23] Recent electron energy loss spectrometry analysis[24] showed that the neutral oxygen deficiency within breakdown path can be as high as 50%, and the vacancies spread out radially from the center of the percolation path. The effect of the oxygen deficiency is simulated in Fig. 1(b) by removing two oxygen atoms in the bulk network of SiO_2, and the selection of the V_O location is according to the scanning transmission electron microscopy cross-section view of the breakdown path.[24] The periodic boundary conditions are

a)Electronic mail: wangbiao@mail.sysu.edu.cn.

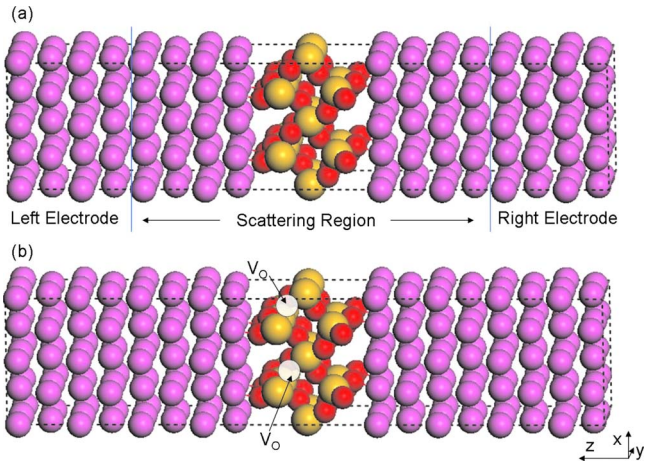

FIG. 1. (Color online) (a) Illustration of the Al–SiO_2–Al system. The golden balls represent Si atoms while red ones represent O atoms; the Al electrode atoms are plotted in purple balls. (b) The white dotted circles indicate the oxygen vacancy in the silica insulator at the scattering area.

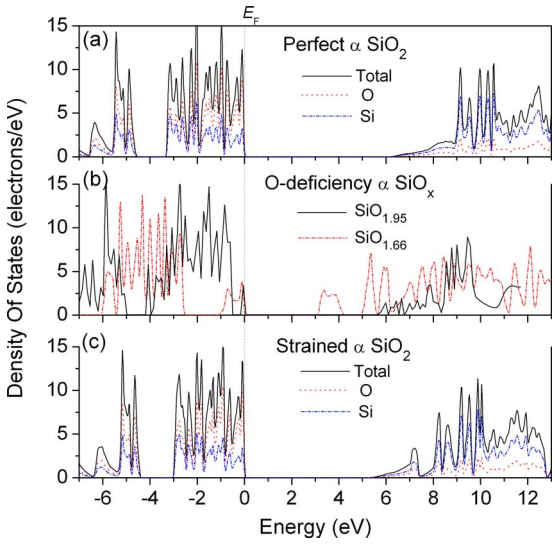

FIG. 2. (Color online) Dependence of the total DOS on the electron energy for (a) optimized perfect α SiO_2, (b) oxygen deficient silica, and (c) the tensile strain α SiO_2. The Fermi level is set to zero.

imposed in the directions parallel to the interface (x and y directions) for the two-probe system. The atomic structure, electronic states, and electron transport properties of the above systems are explored by using the ATOMISTIX TOOLKIT package (ATK 2008.10),[25,26] which combines nonequilibrium Green's function technique with the self-consistent pseudopotential method in the framework of DFT.[27] The exchange correlation potentials are treated by the local density approximation (LDA), and the valence electrons are expanded in a numerical atomic-orbital basis set of single zeta plus polarization. A $18\times18\times80$ k-point mesh is sampled in the surface Brillouin zone according to the Monkhorst–Pack method for the two-probe system. For the transport properties, we found that a denser k-point mesh has little effect on the result.

In the microelectronics industry the silica gate oxide is amorphous, and the short range order of the amorphous SiO_2 is similar to that of the α SiO_2.[28] It is important to note that the disorder effect of amorphous structure will modify the localized valence and conduction band states, which will also influence the carrier mobility.[29] Since the major ideas of this study are focused on the effect of defects in the electronic transport properties, we used the bulk α SiO_2 in the following calculation. As an initial step to clarify the mechanism of leakage current, we first calculated the properties of bulk α SiO_2 and then examined the effect of V_O concentration and electrical stress on the electronic states of bulk α SiO_2.

The optimized lattice constants of α SiO_2 (a =4.815 Å, c=5.338 Å) are about 1.56% smaller than experimental values measured at room temperature.[30] The density of states (DOS) for optimized bulk SiO_2 is given in Fig. 2. It is clear that the top of valence band is primarily composed of O $2p$ states, whereas the bottom of conduction band is dominated by the Si $3p$ character, the mixture of valence states indicating strong covalent bonding. The calculated band gap of the perfect α SiO_2 is 6.3 eV, which is lower than the experimental band gap of about 9 eV but close to the calculated value of 6.4 eV by Sun *et al.*[31] and 5.8 eV by Zhang *et al.*[32] obtained using pseudopotential method within generalized gradient approximation. The underestimate of the band gap can be ascribed to the well known drawback of the approximation used in DFT. The methodological underestimate of the band gap will increase the tunneling current significantly, due to the not well defined band gap problem, only the relative comparison of the tunneling current between the defect structure and the perfect structures makes sense. Using different supercell sizes, the effect of V_O concentration is investigated in Fig. 2(b). There are additional defect states above the valence band maximum for the $SiO_{1.95}$, and the conduction band minimum (CBM) is lowered by 0.6 eV, which is consistent with the experimental observation.[33] With higher V_O concentration, the atomic structure is severely distorted in $SiO_{1.66}$, resulting in more defect states in the band gap and further lower of the CBM. Measurement for dielectric breakdown[24,34] location shows epitaxy configuration induced by electrical stress in Si/SiO_2 interface. Given the importance of the enormous strain field in dielectric breakdown process,[35–37] it is interesting to look at the strain effects on the electronic states. Figure 2(c) shows the DOS information obtained from simulation with 2% tensile strain along the (001) plane of SiO_2. Similar to the effect of oxygen deficiency, the CBM is lowered by about 0.8 eV as compared to the unstrained structure. The DFT simulations also show that the tensile stress in SiO_2 gives relatively high conduction band DOS, which indicates large modification of interfacial carrier mobility at the conduction band edges. Similar effect is found in the strained $Si/Si_{1-x}Ge_x$ devices.[38]

It is noted that the dielectric breakdown behavior is strongly dependent on the SiO_2 configuration and the electrodes with which the field is applied. In the following investigation of I-V characteristics, the influence of electrode is considered by using self-energies calculation. The nonequilibrium electron distribution is described by the nonequilibrium Green's function, which is used to calculate the conductance.[39] The leakage current in a nanoscale device is explored with the Landauer–Büttiker formula:

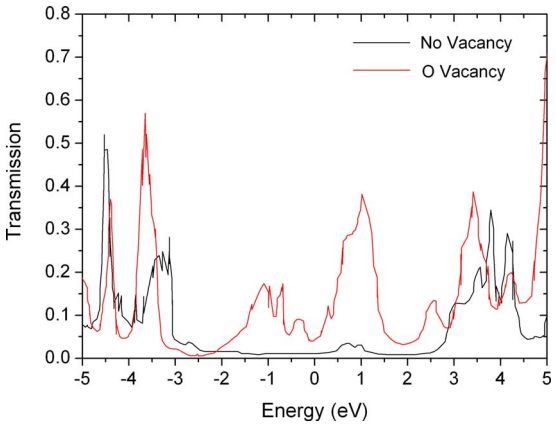

FIG. 3. (Color online) Dependence of the transmission coefficient on the electron energy at zero bias. The Fermi level is set to be the origin of energy.

$$I = \frac{2e}{h}\int T(E)\{n_F(E-\mu_R) - n_F(E-\mu_L)\}dE,$$

where μ_L and μ_R are the chemical potential of the left and right electrode, respectively, n_F is the Fermi distribution function, and $T(E)$ is the transmission probability of electrons passing through the barrier. For zero temperature calculation, the above formula can be written as $(2e/h)\int_{\mu_L}^{\mu_R} T(E)dE$. In Fig. 3, we show the transmission coefficient $T(E,V_b)$ at the zero bias (V_b=0) for the perfect and V_O containing silica junctions given in Fig. 1. It is clear to see that the transmission probability of electrons is strongly enhanced by the introduction of the V_O defect structure. For the perfect silica junction, there exists a molecular band gap ranging from −3 to 3 eV. The gap in the transmission spectra can be contributed to the insulating nature of the silica molecule. On the other hand, the transmission peaks in the oxygen deficient junction are correlated with the active electrical defect states induced by the vacancies. The transmission spectra are consistent with their corresponding DOS distribution discussed above. It is known that the larger the transmission coefficient, the easier it is for an electron to transport across the silica junction. Thus, we display the current as a function of the applied voltage bias for both the perfect and oxygen deficient systems in Fig. 4. At low bias, the leakage currents for both systems show a monotonic increase as the

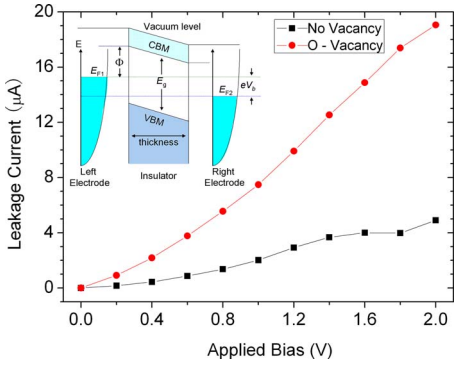

FIG. 4. (Color online) The leakage current as a function of the applied bias for the perfect and oxygen deficient silica junctions. The insert shows the band structure of our model under an applied field. (E_g is the energy gap, E_F is the Fermi energy, V_b is the applied voltage, and Φ is the barrier height)

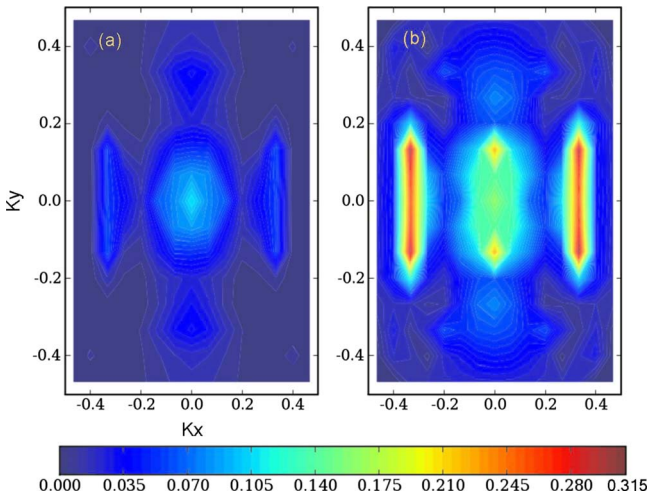

FIG. 5. (Color online) Transmission probability in the two dimensional Brillouin zone of the Al–SiO_2–Al system. (a) shows $K_\parallel$ resolved transmission for the two-probe system with perfect insulator. (b) shows the transmission for the oxygen deficient system with V_O in the barrier.

applied voltage increases. For the oxygen deficient system, it can be written as $I=2.294V+7.014V^2-1.688V^3$, while for the perfect system, it is described by $I=-0.096V+3.194V^2-0.992V^3$. Compared with the experimental sample with 50% oxygen deficiency, the overall calculated leakage currents in our oxygen deficient system is of an order larger than those of measured.[40] The lower of the potential barrier induced by the LDA underestimate of the band gap and the limited simulation thickness can be attributed to the large deviation. The diagram of the band structure under voltage bias is shown in the insert of Fig. 4. Applying a voltage bias at the Al electrodes will shift its Fermi level downwards, which has a profound effect on the band structures. The difference of leakage current for the two systems is obvious, especially at higher voltage bias. The leakage current increases rapidly for oxygen deficient junction, which means the corresponding transmission channels are open and make contribution to the electronic transport. The increment of leakage current in oxygen deficient system is due to the large transmission probability of the V_O defect structure.

The electronic states at the Fermi energy (E_F) determines transport properties. To gain more insight into the large change in leakage current as V_O appeared in barrier, we analyze the $k_\parallel$ resolved transmission for the perfect and oxygen deficient systems at E_F, as plotted in Fig. 5. The features seen for the no vacancy junction in Fig. 5(a) reflect the projection of the transmission probability on the two dimensional Brillouin zone. The main contribution to the transmission comes from the area around the Brillouin zone center at Γ point ($k_\parallel$=0). In the generic quartz, defect-free silica consists of a network of silicon atoms connected via four oxygen bridges to the sp^3 hybridized Si atom, resulting in stiff tetrahedron with a silicon atom in the center and four oxygen atoms at the corners. Once the oxygen vacancy is introduced, the silicon atoms will have one dangling bond and three σ bonds connected to oxygen atoms. The silicon dangling bonds containing trapped electrons (E'_γ) (Ref. 41) will contribute electron DOS at the Fermi surface. As a result, the

transmission peaks for oxygen deficiency systems in Fig. 5(b) are dramatically deformed and enhanced by the defect states. In the mesoscopic and microscopic system, electrical transport takes place through independent conduction channels, which are characterized by a transmission coefficient τ_i, and the total conductance G is the sum of all the contribution of individual conduction channel $\Sigma_i G_0 \tau_i$, where G_0 is the conductance quantum ($7.748\ 091\ 733 \times 10^{-5}$ S). From Fig. 5(b), it is clear to see that four new conduction channels appear at the surrounding of Γ point. Since the conductance across the barrier depends strongly on transmission coefficient, the presence of vacancy defect influences the conductance. Accordingly, the conductance per unit cell changes from $G_{\text{pet}}=0.60$ μS to $G_{V_O}=3.13$ μS when the insulator alters its structure from perfect to oxygen deficient. Therefore, the leakage current of the oxygen deficient system is dominated by these conduction channels. We note that under a reduction condition the V_O has the lowest formation energy,[42] which will cause large leakage current and result in dielectric breakdown of the device. However, the V_O defects will no form easily under an oxidation condition due to their relative large formation energies at the oxygen rich environment. Thus, it is suggested that the dielectric films fabricated under an oxidizing condition will have fewer oxygen vacancies, thus resulting in an extremely low density of Si dangling bonds with high dielectric strength.

In summary, a microscopic physical analysis of the leakage current in silica junction is performed by using first-principles quantum transport calculations. The electron transport and structural properties of the SiO_2 thin film sandwiched between Al electrodes are examined under various external fields. In particular, the effects of oxygen vacancy and electrical stress, which are enormous and often dominate the dielectric breakdown process, are simulated and analyzed in detail. These results show that oxygen vacancy is the key ingredient for the leakage current increment at the atomic level, and a large conductance appeared in the defect structure due to the trapped electrons at the silicon dangling bonds. The large tensile strain field has a similar effect on the band structure as compared to the oxygen vacancies. Since both factors will result in the change in the conduction band edges, it is believed that the electrical strain filed and defect structures are coupled together in the formation of the microscopic conduction path during the breakdown process. It is noted that, in the microelectronic industry, the high-K material and metal gates have been introduced to the complementary metal oxide semiconductor (CMOS) transistors. The metal-oxide gate dielectrics also faced the difficulties caused by defects intrinsic to metal contacts, hopefully, the methodology used in this paper and the calculated results of the $Al/SiO_2/Al$ system can shed light on solving the problem of new high-K material with metal gate.

This work was supported by the National Natural Science Foundation of China (NSFC) (Grant Nos. 10902118, 10831160504, 10572155, and 10732100) and the Research Grants Council of the Hong Kong Special Administrative Region (Grant Nos. G-YX0T, 5322/04E, and N53408).

[1] Y. Zheng and C. H. Woo, J. Phys. D **41**, 175403 (2008).
[2] D. A. Muller, T. Sorsch, S. Moccio, F. H. Baumann, K. Evans-Lutterodt, and G. Timp, Nature (London) **399**, 758 (1999).
[3] T. Choi, S. Lee, Y. J. Choi, V. Kiryukhin, and S. W. Cheong, Science **324**, 63 (2009).
[4] I. Kingon, J. P. Maria, and S. K. Streiffer, Nature (London) **406**, 1032 (2000).
[5] G. D. Wilk, R. M. Wallace, and J. M. Anthony, J. Appl. Phys. **89**, 5243 (2001).
[6] B. H. Lee, L. Kang, R. Nieh, W. J. Qi, and J. C. Lee, Appl. Phys. Lett. **76**, 1926 (2000).
[7] T. H. DiStefano and M. Shatzkes, Appl. Phys. Lett. **25**, 685 (1974).
[8] S. Lombardo, J. H. Stathis, B. P. Linder, K. L. Pey, F. Palumbo, and C. H. Tung, J. Appl. Phys. **98**, 121301 (2005).
[9] V. L. Lo, K. L. Pey, and C. H. Tung, Appl. Phys. Lett. **92**, 012910 (2008).
[10] J. W. Mcpherson, J. Appl. Phys. **99**, 083501 (2006).
[11] P. E. Blochl, Phys. Rev. B **62**, 6158 (2000).
[12] S. J. Wang, Y. F. Dong, Y. P. Feng, and A. C. H. Huan, Microelectron. Eng. **84**, 2332 (2007).
[13] J. H. Stathis, J. Appl. Phys. **86**, 5757 (1999).
[14] T. Tomita, H. Utsunomiya, Y. Kamakura, and K. Taniguchi, Appl. Phys. Lett. **71**, 3664 (1997).
[15] J. W. McPherson and H. C. Mogul, J. Appl. Phys. **84**, 1513 (1998).
[16] L. Niemeyer, L. Pietronero, and H. J. Wiesmann, Phys. Rev. Lett. **52**, 1033 (1984).
[17] J. Sune, I. Placencia, N. Barniol, E. Farres, F. Martin, and X. Aymerich, Thin Solid Films **185**, 347 (1990).
[18] R. Degraeve, G. Groeseneken, R. Bellens, M. Depas, and H. E. Maes, Tech. Dig.- Int. Electron Devices Meet. **1995**, 866 (1995).
[19] J. Junquera and P. Ghosez, Nature (London) **422**, 506 (2003).
[20] R. S. Liu, L. Michalak, C. M. Canali, L. Samuelson, and H. Pettersson, Nano Lett. **8**, 848 (2008).
[21] H. Imai, K. Arai, and H. Imagawa, Phys. Rev. B **38**, 12772 (1988).
[22] S. Agnello, R. Boscaino, G. Buscarino, M. Cannas, and F. M. Gelardi, Phys. Rev. B **66**, 113201 (2002).
[23] J. H. Stathis, IBM J. Res. Dev. **46**, 265 (2002).
[24] X. Li, C. H. Tung, and K. L. Pey, Appl. Phys. Lett. **93**, 072903 (2008).
[25] M. Brandbyge, J. Mozos, P. Ordejon, J. Taylor, and K. Stokbro, Phys. Rev. B **65**, 165401 (2002).
[26] J. Taylor, H. Guo, and J. Wang, Phys. Rev. B **63**, 245407 (2001).
[27] M. C. Payne, M. P. Teter, D. C. Allan, T. A. Arias, and J. D. Joannopoulos, Rev. Mod. Phys. **64**, 1045 (1992).
[28] J. Sarnthein, A. Pasquarello, and R. Car, Phys. Rev. Lett. **74**, 4682 (1995).
[29] Y. Tu and J. Tersoff, Phys. Rev. Lett. **84**, 4393 (2000).
[30] G. Will, M. Bellotto, W. Parrish, and M. Hart, J. Appl. Crystallogr. **21**, 182 (1988).
[31] Q. Sun, Q. Wang, Y. Kawazoe, and P. Jena, Nanotechnology **15**, 260 (2004).
[32] G. Zhang, X. Li, C. H. Tung, K. L. Pey, and G. Q. Lo, Appl. Phys. Lett. **93**, 022901 (2008).
[33] X. Li, C. H. Tung, and K. L. Pey, Appl. Phys. Lett. **93**, 262902 (2008).
[34] C. H. Tung, K. L. Pey, L. J. Tang, M. K. Radhakrishnan, W. H. Lin, F. Palumbo, and S. Lombardo, Appl. Phys. Lett. **83**, 2223 (2003).
[35] K. L. Pey, C. H. Tung, M. K. Radhakrishnan, L. J. Tang, and W. H. Lin, IEDM Tech. Dig.-Int. Electron Devices Meet. **2002**, 163 (2002).
[36] S. Jeffery, C. J. Sofield, and J. B. Pethica, Appl. Phys. Lett. **73**, 172 (1998).
[37] Y. S. Choi, H. Park, T. Nishida, and S. E. Thompson, J. Appl. Phys. **105**, 044503 (2009).
[38] X. Y. Liu, D. Jovanovic, and R. Stumpf, Appl. Phys. Lett. **86**, 082104 (2005).
[39] S. Datta, *Electronic Transport in Mesoscopic Systems* (Cambridge University Press, Cambridge, 1995).
[40] X. Li, C. H. Tung, K. L. Pey, and V. L. Lo, Appl. Phys. Lett. **94**, 132904 (2009).
[41] C. M. Nelson and R. A. Weeks, J. Am. Ceram. Soc. **43**, 396 (1960).
[42] A. Pasquarello, Appl. Surf. Sci. **166**, 451 (2000).